

Low-temperature plasma enhanced atomic layer deposition of large area HfS_2 nanocrystal thin films

Ailing Chang(常爱玲), Yichen Mao(毛亦琛), Zhiwei Huang(黄志伟), Haiyang Hong(洪海洋), Jianfang Xu(徐剑芳), Wei Huang(黄巍), Songyan Chen(陈松岩), Cheng Li(李成)

Citation: Chin. Phys. B . 2020, 29(3): 038102 . **doi:** 10.1088/1674-1056/ab6c4a

Journal homepage: http://cpb.iphy.ac.cn; http://iopscience.iop.org/cpb

What follows is a list of articles you may be interested in

Crystalline silicon surface passivation investigated by thermal atomic-layer-deposited aluminum oxide

Cai-Xia Hou(侯彩霞), Xin-He Zheng(郑新和), Rui Jia(贾锐), Ke Tao(陶科), San-Jie Liu(刘三姐), Shuai Jiang(姜帅), Peng-Fei Zhang(张鹏飞), Heng-Chao Sun(孙恒超), Yong-Tao Li(李永涛)

Chin. Phys. B . 2017, 26(9): 098103 . **doi:** 10.1088/1674-1056/26/9/098103

Influences of annealing on structural and compositional properties of Al_2O_3 thin films grown on 4H-SiC by atomic layer deposition

Li-Xin Tian(田丽欣), Feng Zhang(张峰), Zhan-Wei Shen(申占伟), Guo-Guo Yan(闫果果), Xing-Fang Liu(刘兴昉), Wan-Shun Zhao(赵万顺), Lei Wang(王雷), Guo-Sheng Sun(孙国胜), Yi-Ping Zeng(曾一平)

Chin. Phys. B . 2016, 25(12): 128104 . **doi:** 10.1088/1674-1056/25/12/128104

Atomic-layer-deposited Al_2O_3 and HfO_2 on InAlAs: A comparative study of interfacial and electrical characteristics

Li-Fan Wu(武利翻), Yu-Ming Zhang(张玉明), Hong-Liang Lv(吕红亮), Yi-Men Zhang(张义门)

Chin. Phys. B . 2016, 25(10): 108101 . **doi:** 10.1088/1674-1056/25/10/108101

Influences of different structures on the characteristics of H_2O-based and O_3-based La_xAl_yO films deposited by atomic layer deposition

Chen-Xi Fei(费晨曦), Hong-Xia Liu(刘红侠), Xing Wang(汪星), Dong-Dong Zhao(赵冬冬), Shu-Long Wang(王树龙), Shu-Peng Chen(陈树鹏)

Chin. Phys. B . 2016, 25(5): 058106 . **doi:** 10.1088/1674-1056/25/5/058106

Effects of annealing temperature on shape transformation and optical properties of germanium quantum dots

Alireza Samavati, Z. Othaman, S. K. Ghoshal, M. K. Mustafa

Chin. Phys. B . 2015, 24(2): 028103 . **doi:** 10.1088/1674-1056/24/2/028103

Low-temperature plasma enhanced atomic layer deposition of large area HfS_2 nanocrystal thin films*

Ailing Chang(常爱玲)[1], Yichen Mao(毛亦琛)[1], Zhiwei Huang(黄志伟)[2], Haiyang Hong(洪海洋)[1], Jianfang Xu(徐剑芳)[1], Wei Huang(黄巍)[1], Songyan Chen(陈松岩)[1], and Cheng Li(李成)[1,†]

[1] *Department of Physics, OSED, Semiconductor Photonics Research Center, Xiamen University, Xiamen* 361005, *China*
[2] *Xiamen University Tan Kah Kee College, Zhangzhou* 363105, *China*

(Received 10 December 2019; revised manuscript received 9 January 2020; accepted manuscript online 16 January 2020)

Hafnium disulfide (HfS_2) is a promising two-dimensional material for scaling electronic devices due to its higher carrier mobility, in which the combination of two-dimensional materials with traditional semiconductors in the framework of CMOS-compatible technology is necessary. We reported on the deposition of HfS_2 nanocrystals by remote plasma enhanced atomic layer deposition at low temperature using $Hf(N(CH_3)(C_2H_5))_4$ and H_2S as the reaction precursors. Self-limiting reaction behavior was observed at the deposition temperatures ranging from 150 °C to 350 °C, and the film thickness increased linearly with the growth cycles. The uniform HfS_2 nanocrystal thin films were obtained with the size of nanocrystal grain up to 27 nm. It was demonstrated that higher deposition temperature could enlarge the grain size and improve the HfS_2 crystallinity, while causing crystallization of the mixed HfO_2 above 450 °C. These results suggested that atomic layer deposition is a low-temperature route to synthesize high quality HfS_2 nanocrystals for electronic device or electrochemical applications.

Keywords: HfS_2, atomic layer deposition, surface morphology

PACS: 81.07.Bc, 81.15.Gh **DOI:** 10.1088/1674-1056/ab6c4a

1. Introduction

Two-dimensional (2D) transition metal dichalcogenides (TMDs) are considered as promising candidate materials for optoelectronic devices because of their fascinating electronic, optical, and mechanical properties.[1–5] As a member of TMDs family, hafnium disulfide (HfS_2) is a layered material in which the layers are connected by weak van der Waals forces and Hf and S atoms in the layers are connected by strong chemical bonds. HfS_2 possesses ultrahigh room-temperature carrier mobility, which is necessary for the realization of high-performance electronic devices.[6] However, instability of HfS_2 makes it more difficult to synthesis and be applied in atmosphere ambient. Environmental sensitivity study performed on HfS_2 proves that oxidation due to moisture and oxygen adsorption occurs quickly.[7,8]

Controllable synthesis of TMDs is necessary for obtaining high quality, uniform, atomic thin films to realize business application. Currently, the synthesis methods of two-dimensional materials are mainly divided into top-down methods (such as mechanical exfoliation and chemical exfoliation) and bottom-up methods (such as chemical vapor deposition and atomic layer deposition).[4,9] In current scientific research, most of the 2D TMDs have been obtained by means of mechanical exfoliation, in which single-layer or few layers of HfS_2 are divided by a tape. HfS_2 layers obtained by mechanical exfoliation have high quality, but low yield and poor repeatability, making it difficult to obtain large size films. HfS_2 films with large size and high uniformity can be achieved by chemical vapor deposition using $HfCl_4$ powders and sulfur pieces or sulfur powders.[10–17] However, the growth temperature of chemical vapor deposition is high, and the quality of the films is greatly affected by the environment inside the reaction chamber.

As a special chemical vapor deposition method, the atomic layer deposition (ALD) has a growth temperature below 500 °C, so it is well compatible with the complementary metal–oxide–semiconductor (CMOS) process. ALD is an indispensable method to combine two-dimensional materials with traditional semiconductors. In addition, ALD has unique self-limiting reaction mechanism, which can grow films with high uniformity, high shape preserving, and precise thickness control. Therefore, ALD has been widely used in the synthesis of 2D TMDs, such as MoS_2,[18–26] WS_2,[27–29] SnS_2,[30,31] and ReS_2.[32,33] So far, HfS_2 and ZrS_2 thin films have been deposited by ALD using $HfCl_4$ and $ZrCl_4$ with H_2S as the precursors.[34]

In this work, we synthesized HfS_2 films by remote plasma enhanced atomic layer deposition (RPALD) at lower temperature, with $Hf[(C_2H_5)(CH_3)N]_4$ (TEMAH) and H_2S as the reaction precursors. The influence of the deposition temperature on the surface morphology and crystallinity of HfS_2 thin films were analyzed by various characterization techniques. The temperature range of self-limiting reaction behavior and the growth rate were determined. The uniform HfS_2 nanocrystals

*Project supported by the National Key Research and Development Program of China (Grant No. 2018YFB2200103).
†Corresponding author. E-mail: lich@xmu.edu.cn
© 2020 Chinese Physical Society and IOP Publishing Ltd

were deposited on sapphire, thermally oxidized 300 nm thick silicon dioxide layer (SiO_2/Si), and silicon (Si) substrates, respectively, and characterized by Raman and x-ray diffraction. The HfS_2 film mixed with hafnium dioxide (HfO_2) was distinguished, which was easily oxidized under ambient conditions.

2. Experimental details

2.1. Synthesis of HfS_2 films by RPALD

HfS_2 thin films were deposited in a commercial PRALD setup (R200 Advanced) from PICOSUN. The growth was performed on diverse substrates: sapphire, SiO_2/Si, and Si. Sapphire and 300 nm SiO_2/Si substrates were cleaned by acetone, ethanol, and deionized water in an ultrasonic bath for three times. Si was cleaned by boiled H_2SO_4/H_2O_2 (4 : 1) for 10 min, then etched by HF/H_2O (1 : 20) for 4 min, and washed in deionized water. The Hf precursor employed was TEMAH, which was heated to 120 °C and delivered to the reactor chamber at 130 °C. H_2S (3.5%, balance Ar) with a flow rate of 150 standard cubic centimeter per minute (sccm) was used as the S source. A remote plasma source operating at the power of 1000 W was used for the H_2S plasma step. The deposition temperature was varied from 150 °C to 500 °C and the chamber pressure was controlled at 6 hundred Pa (hPa), regardless of the deposition temperature. Two precursors were alternately exposed to the substrates and subsequently purged for each precursor in an ALD cycle. One growth cycle consists of four main steps: (i) 1.6 s exposure to TEMAH, (ii) 10 s N_2 purge, (iii) 10 s exposure to H_2S, (iv) 10 s N_2 purge. By repeating these steps, HfS_2 thin films with desired layers can be obtained. The possible reaction is as follows:

$$\mathrm{Hf[(C_2H_5)(CH_3)N]_4(g) + 2H_2S(g)} = \mathrm{HfS_2(s) + 4\,(C_2H_5)(CH_3)NH(g)}.$$

2.2. Characterization

The thickness of the HfS_2 films was measured by x-ray reflectivity using a PANalytical instrument. Atomic force microscope (AFM) was performed with tapping mode on a SPA400-Nanonavi instrument. Raman spectra were measured with 532 nm excitation under ambient conditions using ID-Spec ARCTIC, and the power levels on the sample were 0.1 mW. The x-ray diffraction (XRD) was performed on a Rigaku IV instrument. The x-ray photoelectron spectroscopy (XPS) was performed on a PHI Quantum-2000 instrument, and a conventional Al $K\alpha$ anode was used as the source of x-ray radiation.

3. Results and discussion

3.1. Self-limiting growth and thickness control

The self-limiting growth behavior of the ALD process for HfS_2 thin films was investigated at temperatures ranging from 150 °C to 500 °C. Figure 1(a) shows the variation in the growth rate of HfS_2 films as a function of temperature. The HfS_2 film thickness was evaluated via x-ray reflectivity measurement. A saturated growth rate per cycle (GPC) of about 0.11 nm was estimated at temperatures ranging from 150 °C to 350 °C. When the growth temperature was higher than 450 °C, the growth rate started to surge from 0.17 nm to 0.8 nm per cycle at 500 °C. Therefore, the ALD temperature window between 150 °C and 350 °C for the growth of ALD-HfS_2 using TEMAH and remote H_2S plasma was confirmed. Figure 1(b) shows the variation in the thickness of the HfS_2 films grown at 250 °C as a function of the number of cycles. Under basic pulsing conditions, the number of reaction cycles was varied from 80 to 500. The film thickness roughly linearly increases with the number of cycles, and the GPC is calculated to be 0.11 nm per cycle from the slope of the linear fit.

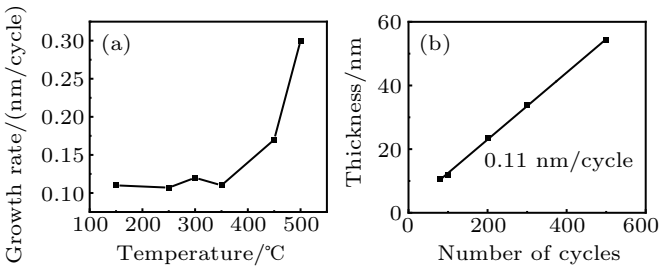


Fig. 1. (a) Variation in the growth rate of HfS_2 films as a function of temperature. (b) Variation in the thickness of HfS_2 films grown at 250 °C as a function of the number of cycles.

3.2. Surface morphology

The optical images of samples grown on 300 nm SiO_2/Si, sapphire, and Si substrates by RPALD are shown in Fig. 2. At different growth temperatures, the surface colors of the HfS_2 films are uniform and slightly different, and they are all different from those of the bare substrates. Along with the increase of the growth temperature, the colors of the HfS_2 films on 300 nm SiO_2/Si wafer (Figs. 2(a)–2(e)) uniformly change from dark yellow green to light yellow green, and then to dark yellow green again. For the HfS_2 films deposited on sapphire wafer (Figs. 2(f)–2(j)), the colors change from transparency to a slight tan. For the HfS_2 films deposited on Si wafer (Figs. 2(k)–2(o)), the colors also change to brown compared with the bare Si substrate. It is visibly clear that the deposited HfS_2 films are continuous and uniformly flat across the wafer.

We also examined the surface morphology of the HfS_2 films by AFM and SEM measurements. The AFM images of the as-grown HfS_2 films deposited on Si substrates for 100 cycles at various temperatures are shown in Figs. 3(a)–3(c). The surface of all HfS_2 films is uniform and smooth with similar surface morphology. The root-mean-square (RMS) surface roughness of the HfS_2 films slightly increases from 0.32 nm to 0.76 nm with increasing growth temperature from 250 °C to 450 °C. Figures 3(d)–3(f) show the SEM images of the HfS_2

films deposited on Si for 100 cycles at 250 °C, 350 °C, and 450 °C, respectively. Small grains in the smooth surface are observed for all the HfS_2 films, indicating that the continuous and uniform HfS_2 films are deposited in the self-limiting growth window.

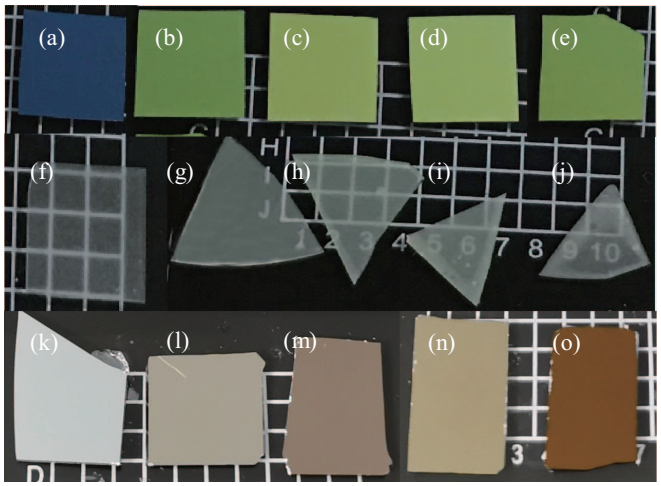


Fig. 2. Optical images of the HfS_2 films deposited for 300 cycles on 300 nm SiO_2/Si, sapphire, and Si substrates. (a) Bare 300 nm SiO_2/Si; HfS_2 films deposited on SiO_2/Si at (b) 150 °C, (c) 250 °C, (d) 350 °C, (e) 450 °C; (f) bare sapphire; HfS_2 films deposited on sapphire at (g) 150 °C, (h) 250 °C, (i) 350 °C, (j) 450 °C; (k) bare Si; HfS_2 films deposited on Si at (l) 150 °C, (m) 250 °C, (n) 350 °C, (o) 450 °C.

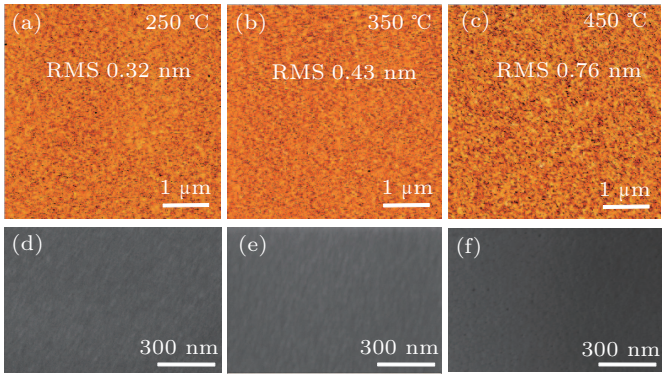


Fig. 3. AFM images of the HfS_2 films deposited on Si for 100 cycles at (a) 250 °C, (b) 350 °C, and (c) 450 °C. SEM images of the HfS_2 films deposited on Si for 100 cycles at (d) 250 °C, (e) 350 °C, and (f) 450 °C.

In order to study the effect of substrate on the surface morphology of the deposited HfS_2 films, the AFM images of the samples grown on Si and sapphire substrates are compared. Figures 4(a)–4(d) show the 500 nm×500 nm AFM images of the HfS_2 films deposited on Si and sapphire substrates at 450 °C for 80 cycles and 300 cycles, respectively. The surface of the HfS_2 films on both Si and sapphire substrates becomes rougher with the thickness increasing from 13.6 nm (80 cycles) to 51.0 nm (300 cycles), indicating that the grain size increases with HfS_2 thickness obviously. Figure 4(e) shows the grain size statistical distribution of the HfS_2 deposited for 80 cycles and 300 cycles on Si and sapphire. The grain size of HfS_2 is mainly distributed in 15–25 nm for 80 cycles and 20–30 nm for 300 cycles. The average grain size of HfS_2 increases from 22.3 nm to 27.1 nm for the samples deposited for 80 cycles and 300 cycles on Si, and from 22.2 nm to 24.1 nm for the samples on sapphire.

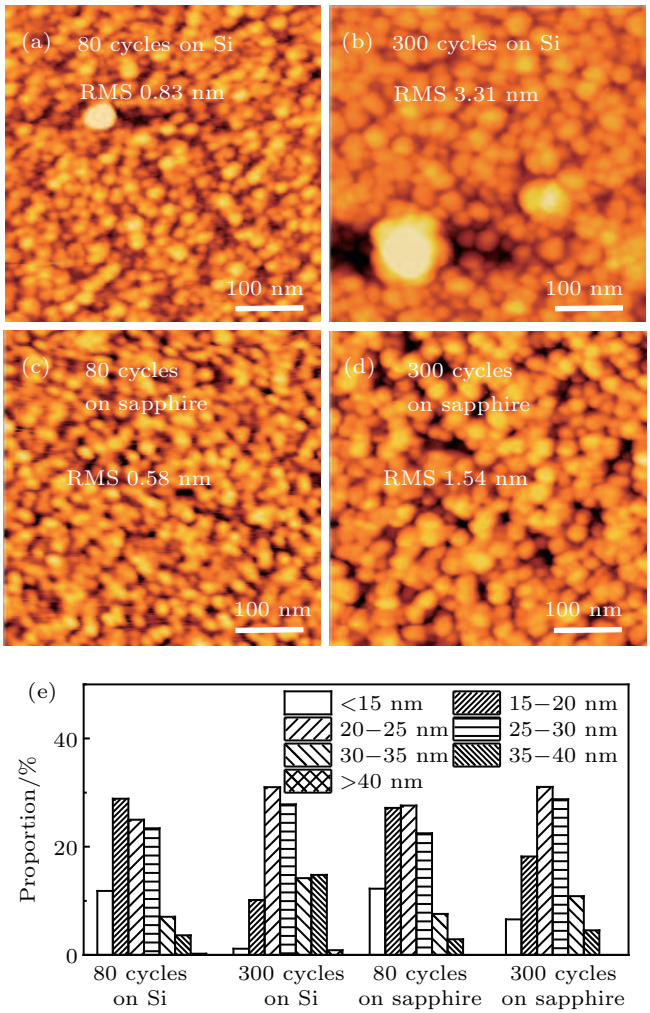


Fig. 4. AFM images of the HfS_2 films deposited at 450 °C for (a) 80 cycles on Si; (b) 300 cycles on Si; (c) 80 cycles on sapphire; (d) 300 cycles on sapphire. (e) Grain size statistical distribution of the HfS_2 deposited for 80 cycles and 300 cycles on Si and sapphire.

3.3. Chemical composition

Auger electron spectroscopy was used to analyze the element fraction in the HfS_2 thin films. Figure 5 shows the depth

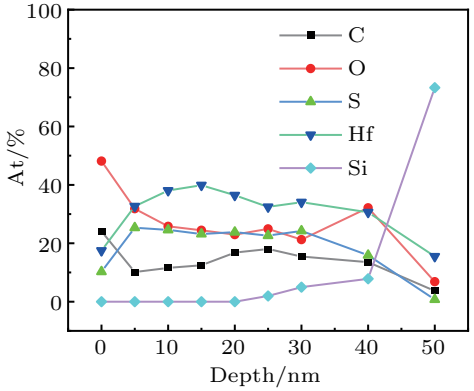


Fig. 5. Depth profile of elements in the HfS_2 film deposited on Si at temperature of 350 °C for 300 cycles.

profile of elements in the HfS_2 films deposited at 350 °C for 300 cycles. The oxygen content on the surface is much higher than that in the inside, suggesting that oxidation of HfS_2 easily occurs under ambient conditions. With the depth changing from 10 nm to 30 nm, the element contents of Hf, S, and O basically keep constant. The atomic percentages of Hf, O, and S are about 35%, 25%, and 25%, respectively. It indicates that the deposited films under this condition have some HfO_2 mixing in HfS_2. The content of Si starts increasing dramatically at the depth of 30 nm, indicating that the HfS_2 film thickness is about 30 nm, which is consistent with the deposited film thickness (33 nm) measured by x-ray reflectivity.

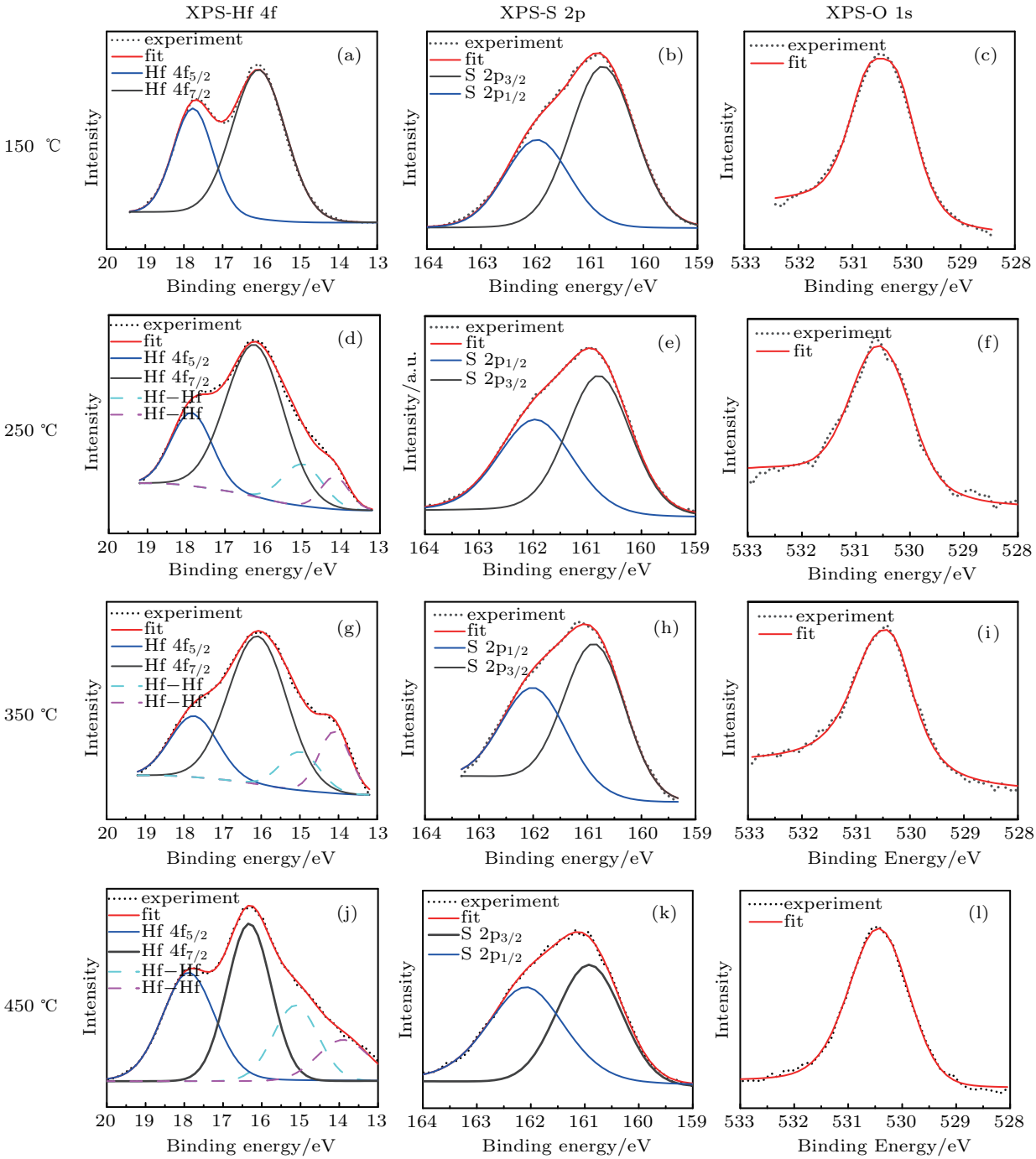


Fig. 6. XPS core-level spectra of the ALD-HfS_2 films prepared by 80 ALD cycles at (a)–(c) 150 °C, (d)–(f) 250 °C, (g)–(i) 350 °C, and (j)–(l) 450 °C: (a), (d), (g), (j) Hf 4f; (b), (e), (h), (k) S 2p; (c), (f), (i), (l) O 1s.

In order to further determine the chemical states of Hf, S, and O in the films, XPS was used to evaluate the formation of chemical bonding in the HfS_2 films. To remove oxidation of the surface, 5 nm HfS_2 films on the surface were etched away by Ar ions. The XPS spectra of the surface and at 5 nm depth of the HfS_2 films were tested. Figure 6 shows the XPS spectra at 5 nm depth of the HfS_2 films grown for 80 cycles at 150 °C, 250 °C, 350 °C, and 450 °C, respectively. For the XPS spectra of the HfS_2 film deposited at 150 °C, Hf $4f_{7/2}$ and Hf $4f_{5/2}$ components are found at 16.1 eV and

17.8 eV (Fig. 6(a)), respectively. A broad feature appears in the S 2p region with $2p_{3/2}$ and $2p_{1/2}$ components at 160.9 eV and 162.1 eV (Fig. 6(b)), respectively. These features are consistent with the HfS_2 peak positions reported previously.[10,11] The O 1s peaks at 530.4 eV binding energy are associated with HfO_2,[27] as shown in Fig. 6(c). However, compared with that of Hf 4f bonding to S, the spectra of Hf–O bond (near 19.1 eV)[10] is too small to be detected. For the XPS spectra of the HfS_2 film deposited at 250 °C, in addition to the Hf–S spectra, the peaks at 14.1 eV and 15.2 eV (Fig. 6(d)) binding energy are attributed to the Hf–Hf bond,[35] which are introduced by the Ar ion etching process. Figure 6(e) shows the binding energy of S 2p bonding to S, and figure 6(f) shows the binding energy of O 1s bonding to Hf. Similarly, the XPS spectra of the HfS_2 films grown at 350 °C (Figs. 6(g)–6(i)) and 450 °C (Figs. 6(j)–6(l)) show the same characteristics as those grown at 250 °C. The full XPS spectra demonstrate that the as-grown HfS_2 films are of correct chemical composition but mixed with HfO_2.

Table 1. Atomic percentages of Hf, S, and O in HfS_2 thin films evaluated by the sensitivity factor method from XPS.

	Surface			Etching 5 nm		
Deposition temperature	Hf/%	S/%	O/%	Hf/%	S/%	O/%
150 °C	21.211	25.816	52.974	22.765	51.890	25.345
250 °C	18.869	36.817	44.314	20.389	70.512	09.100
350 °C	20.139	42.732	37.129	24.673	54.622	20.705
450 °C	27.680	19.175	53.146	31.243	25.400	43.357

According to the XPS measurement of the surface and at 5 nm depth of the HfS_2 films, the atomic percentages of Hf, S, and O in the HfS_2 thin films were evaluated by the sensitivity factor method, and the results are listed in Table 1. The Hf content is approximately 25% and the element contents of S and O in total are around 75%, suggesting the mixture of HfO_2 and HfS_2. The element content of S at 5 nm depth of the HfS_2 films is higher than that at the surface, while the element content of O at the surface of the HfS_2 films is much higher than that at 5 nm depth. These results suggest that the as-deposited HfS_2 is easily oxidized in the atmosphere. The S content in the films deposited at less than 450 °C is much higher than the O content, indicating that HfS_2 is the dominant component in the films. Almost pure HfS_2 films can be obtained at 250 °C. When the deposition temperature is as high as 450 °C, the HfS_2 films become oxygen-rich. Oxygen incorporation mechanism and suppression need further investigation.

3.4. Film crystallinity

Raman spectra of the HfS_2 films grown on SiO_2/Si for 300 cycles at various temperatures are shown in Fig. 7(a). Besides the peaks from the Si substrate (300 cm^{-1}), there are only two peaks located at 260 cm^{-1} and 338 cm^{-1}, corresponding to the in-plane vibrational mode (E^1_{2g}) and out-plane vibrational mode (A_{1g}) of HfS_2, respectively. Strong Raman peaks from the HfS_2 films deposited at the temperatures from 250 °C to 450 °C show the formation of a locally ordered structure. The lack of Raman peaks of both E^1_{2g} and A_{1g} modes for the HfS_2 films deposited at 150 °C suggests that the HfS_2 films are amorphous. Combined with the observation of grains in the SEM and AFM images, it is demonstrated that nanocrystal HfS_2 films are achieved with RPALD at lower temperature down to 250 °C. The grain size of HfS_2 increases with the increase of the thickness and growth temperature. Higher deposition temperature improves the atomic ordering in the HfS_2 films, resulting in significant improvement of intensities of the characteristic E^1_{2g} and A_{1g} modes.

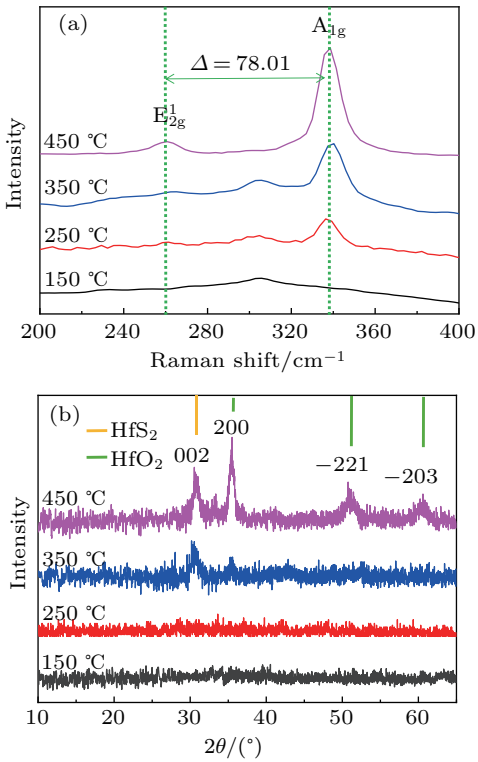


Fig. 7. Film crystallinity of HfS_2 films deposited for 300 cycles. (a) Raman spectra of HfS_2 films deposited at 150–450 °C. (b) GIXRD patterns of HfS_2 films deposited at 150–450 °C.

Grazing incident XRD was also used to study the structural properties and crystalline nature of the HfS_2 films. Grazing incident XRD patterns of the as-grown HfS_2 films with small signal from the oxide phase are shown in Fig. 7(b). There are no diffraction peaks observed for the films deposited

at 150 °C and 250 °C. As the growth temperature increases, HfS_2 films deposited at 350 °C show a crystalline HfS_2 (002) diffraction peak at 30.5° and a weak HfO_2 (200) diffraction peak at 35.6° in the XRD pattern. When the growth temperature increases to 450 °C, besides the enhanced HfS_2 (002) and HfO_2 (200) peaks, two new diffraction peaks appear at 50.8° and 60.4°, corresponding to HfO_2 (−221) and HfO_2 (−203) diffraction peaks, respectively. These results show that the crystallinity of HfS_2 is improved with the increase of the deposition temperature. However, a temperature as higher as 450 °C could also cause the transformation of nanocrystal HfO_2 mixed in the HfS_2 to polycrystalline.

4. Conclusions

In summary, we have successfully deposited HfS_2 nanocrystal thin films by RPALD at low temperature with TEMAH and H_2S as the precursors. Self-limiting growth behavior is observed in the temperature range of 150 °C to 350 °C with a growth rate of about 0.11 nm/cycle. The surface of the deposited HfS_2 is smooth with the appearance of uniformly nanocrystal grains. The size of the nanocrystal grain depends on the growth temperature, the kind of substrate, and the HfS_2 film thickness. The crystalline HfS_2 is achieved at lower temperature down to 250 °C, and the crystal quality is significantly improved with increasing deposition temperature. However, the as-deposited HfS_2 films are almost oxygen-rich, in which crystallized HfO_2 is detected for the sample deposited at higher temperature. In addition, the as-deposited HfS_2 is easily oxidized in the atmosphere. Further investigation is needed to lower the oxygen content and increase the crystallinity of the HfS_2 films. Low temperature atomic layer deposition is believed to be a promising route to large area HfS_2 nanocrystal thin films growth for electronic or electrochemical applications in the future.

References

[1] Butler S Z, Hollen S M, Cao L, Cui Y, Gupta J A, Gutiérrez H R, Heinz T F, Hong S S, Huang J, Ismach A F, Johnston-Halperin E, Kuno M, Plashnitsa V V , Robinson R D, Ruoff R S, Salahuddin S, Shan J, Shi L, Spencer M G, Terrones M, Windl W and Goldberger J E 2013 *ACS Nano* **7** 2898

[2] Wang Q H, Kalantar-Zadeh K, Kis A, Coleman J N and Strano M S 2012 *Nat. Nanotechnol.* **7** 699

[3] Manzeli S, Ovchinnikov D, Pasquier D, Yazyev O V and Kis A 2017 *Nat. Rev. Mater.* **2** 17033

[4] Choi W, Choudhary N, Han G H, Park J, Akinwande D and Lee Y H 2017 *Mater. Today* **20** 116

[5] Duong D L, Yun S J and Lee Y H 2017 *ACS Nano* **11** 11803

[6] Kanazawa T, Amemiya T, Ishikawa A, Upadhyaya V, Tsuruta K, Tanaka T and Miyamoto Y 2016 *Sci. Rep.* **6** 22277

[7] Mirabelli G, McGeough C, Schmidt M, McCarthy E K, Monaghan S, Povey I M, McCarthy M, Gity F, Nagle R, Hughes G, Cafolla A, Hurley P K and Duffy R 2016 *J. Appl. Phys.* **120** 125102

[8] Chae S H, Jin Y, Kim T S, Chung D S, Na H, Nam H, Kim H, Perello D J, Jeong H Y, Ly T H and Lee Y H 2016 *ACS Nano* **10** 1309

[9] Wang D, Zhang X and Wang Z 2018 *J. Nanosci. Nanotechnol.* **18** 7319

[10] Yan C, Gan L, Zhou X, Guo J, Huang W, Huang J, Jin B, Xiong J, Zhai T and Li Y 2017 *Adv. Funct. Mater.* **27** 1702918

[11] Wang D, Zhang X, Liu H, Meng J, Xia J, Yin Z, Wang Y, You J and Meng X M 2017 *2D Mater.* **4** 031012

[12] Fu L, Wang F, Wu B, Wu N, Huang W, Wang H, Jin C, Zhuang L, He J, Fu L and Liu Y 2017 *Adv. Mater.* **29** 1700439

[13] Kaur H, Yadav S, Srivastava A K, Singh N, Rath S, Schneider J J, Sinha O P and Srivastava R 2018 *Nano Res.* **11** 343

[14] Zheng B, Chen Y, Wang Z, Qi F, Huang Z, Hao X, Li P, Zhang W and Li Y 2016 *2D Mater.* **3** 035024

[15] Wang D, Meng J, Zhang X, Guo G, Yin Z, Liu H, Cheng L, Gao M, You J and Wang R 2018 *Chem. Mater.* **30** 3819

[16] Zheng B, Wang Z, Qi F, Wang X, Yu B, Zhang W and Chen Y 2018 *Appl. Surf. Sci.* **435** 563

[17] Brooks D J, Douthwaite R E, Brydson R, Calvert C, Measures M G and Watson A 2006 *Nanotechnology* **17** 1245

[18] Oh S, Kim J B, Song J T, Oh J and Kim S H 2017 *J. Mater. Chem. A* **5** 3304

[19] Huang Y, Liu L and Liu X 2019 *Nanotechnology* **30** 95402

[20] Nandi D K, Sen U K, Choudhury D, Mitra S and Sarkar S K 2014 *Electrochim. Acta* **146** 706

[21] Jin Z, Shin S, Kwon D H, Han S J and Min Y S 2014 *Nanoscale* **6** 14453

[22] Kwon D H, Jin Z, Shin S, Lee W S and Min Y S 2016 *Nanoscale* **8** 7180

[23] Xiong D, Zhang Q, Li W, Li J, Fu X, Cerqueira M F, Alpuim P and Liu L 2017 *Nanoscale* **9** 2711

[24] Kim H J, Jeon H and Shin Y H 2018 *J. Appl. Phys.* **124** 115301

[25] Shimizu J, Ohashi T, Matsuura K, Muneta I, Kuniyuki K, Tsutsui K, Ikarashi N and Wakabayashi H 2019 *IEEE J. Electron. Devices Soc.* **7** 76

[26] Hao W, Marichy C and Journet C 2019 *2D Mater.* **6** 012001

[27] Groven B, Mehta A N, Bender H, Smets Q, Meersschaut J, Franquet A, Conard T, Nuytten T, Verdonck P, Vandervorst W, Heyns M, Radu I, Caymax M and Delabie A 2018 *J. Vac. Sci. Technol. A Vac. Surf. Film* **36** 01A105

[28] Wu Y, Raza M H, Chen Y C, Amsalem P, Wahl S, Skrodczky K, Xu X, Lokare K S, Zhukush M, Gaval P, Koch N, Quadrelli E A and Pinna N 2019 *Chem. Mater.* **31** 1881

[29] Yeo S, Nandi D K, Rahul R, Kim T H, Shong B, Jang Y, Bae J S, Han J W, Kim S H and Kim H 2018 *Appl. Surf. Sci.* **459** 596

[30] Pyeon J J, Baek I H, Lim W C, Chae K H, Han S H, Lee G Y, Baek S H, Kim J S, Choi J W, Chung T M, Han J H, Kang C Y and Kim S K 2018 *Nanoscale* **10** 17712

[31] Lee N, Lee G, Choi H, Park H, Choi Y, Kim K, Choi Y, Kim J W, Yuk H, Sul O, Lee S B and Jeon H 2019 *Appl. Surf. Sci.* **496** 143689

[32] Lv J and Liu L 2020 *Nanotechnology* **31** 055602

[33] Hämäläinen J, Mattinen M, Mizohata K, Meinander K, Vehkamäki M, Räisänen J, Ritala M and Leskelä M 2018 *Adv. Mater.* **30** 1703622

[34] Mattinen M, Popov G, Vehkamäki M, King P J, Mizohata K, Jalkanen P, Räisänen J, Leskelä M and Ritala M 2019 *Chem. Mater.* **31** 5713

[35] Chi X, Lan X, Lu C, Hong H, Li C, Chen S, Lai H, Huang W and Xu J 2016 *Mater. Res. Express* **3** 035012